Analysis of Dielectric Breakdown of Hot SF_6 Gas in a Gas Circuit Breaker

Hong-Kyu Kim†, Jin-Kyo Chong* and Ki-Dong Song**

Abstract – This paper presents the analysis of the dielectric characteristics of a hot SF_6 gas in a gas circuit breaker. Hot gas flow is analyzed using the FVFLIC method considering the moving boundary, material properties of real SF_6 gas, and arc plasma. In the arc model, the re-absorption of the emitted radiation is approximated with the boundary source layer where the re-absorbed radiation energy is input as an energy source term in the energy conservation equation. The breakdown criterion of a hot gas is predicted using the critical electric field as a function of temperature and pressure. To validate the simulation method, breakdown voltage for a 145kV 40kA circuit breaker was measured for various conditions. Consistent results between the simulation and experiment were confirmed.

Keywords: Gas circuit breaker, Hot SF_6 gas, Dielectric breakdown, Critical electric field, Arc plasma

1. Introduction

During a large current interruption, hot gas flow is formed inside the high voltage gas circuit breaker (GCB) due to the arc plasma generated between the arcing contacts. As shown in Fig. 1, when the hot gas flow reaches between a tank and a shield, the high temperature and low density gas results in the reduction in the dielectric withstand. Moreover, when the transient recovery voltage (TRV) approaches its peak value after a current interruption, the possibility of a breakdown becomes high. These days, the reduction in dielectric strength under hot gas conditions is one of the crucial problems to be resolved in the design of a compact GCB [1]-[2].

In this paper, we present the prediction method of dielectric breakdown after a large current interruption in a GCB. The prediction procedure is composed of the hot gas flow analysis, electric field analysis, and the calculation of the critical electric field intensity as shown in Fig. 2. The hot gas flow is analyzed using the FVFLIC (finite volume fluid in cell) method [3] which can consider the compressible and supersonic flow. The arc is simulated as an energy source term in the energy conservation equation.

The breakdown voltage is predicted using the critical electric field intensity. Much research has been carried out to calculate the critical breakdown field strength [4]-[6]. We employ the $(E/N)_c$ data derived by Yousfi [6] to obtain the critical electric field intensity E_{cr}. The prediction method is applied to the 145kV GCB model and the simulation results are compared with the experimental ones.

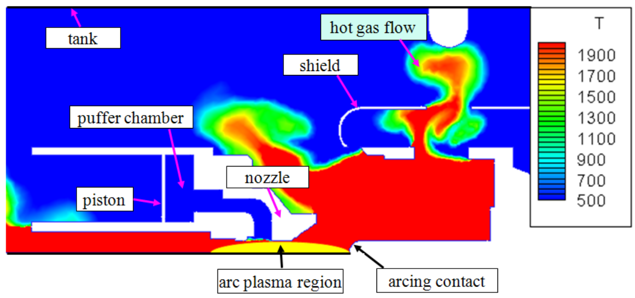

Fig. 1. Geometry of GCB and hot gas distribution during large current interruption.

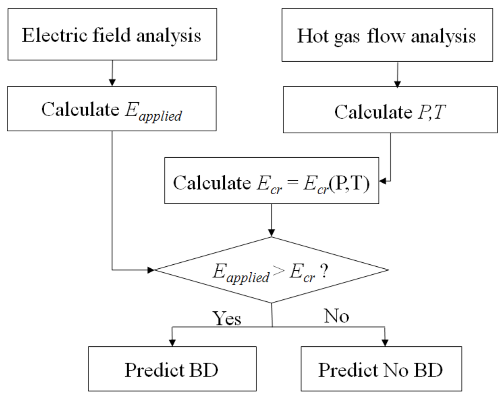

Fig. 2. Procedure of dielectric breakdown prediction (BD:breakdown).

2. Hot Gas Flow Analysis

Many researchers agree that the arc plasma can be treated as the local thermodynamic equilibrium condition. Therefore, the classical conservation equations for mass, momentum and energy can be used to analyze the hot gas flow considering the interaction with the arc plasma.

† Corresponding Author: Korea Electrotechnology Research Institute, Korea. (kimhk@keri.re.kr)
* Korea Electrotechnology Research Institute, Korea. (jkchong@keri.re.kr)
** Korea Electrotechnology Research Institute, Korea. (kdsong@keri.re.kr)
Received: January 16, 2009; Accepted: March 12, 2010

Many physical phenomena should be taken into account for the accurate analysis of the interaction between gas flow and arc plasma, such as moving geometry, compressible flow, joule heating, arc radiation, electric and magnetic effect, wall ablation, electrode melting, and so on. In this study, the effects of magnetic force, nozzle ablation, and electrode melting are not considered. The non-viscous and compressible flow is solved in the axisymmetric geometry with the following conservation equations:

$$\frac{\partial \rho}{\partial t} + \frac{\partial(\rho ur)}{r\partial r} + \frac{\partial(\rho v)}{\partial z} = 0 \quad (1)$$

$$\frac{\partial(\rho u)}{\partial t} + \frac{\partial(\rho u^2 r)}{r\partial r} + \frac{\partial(\rho uv)}{\partial z} = -\frac{\partial(pr)}{r\partial r} \quad (2)$$

$$\frac{\partial(\rho v)}{\partial t} + \frac{\partial(\rho uvr)}{r\partial r} + \frac{\partial(\rho v^2)}{\partial z} = -\frac{\partial p}{\partial z} \quad (3)$$

$$\frac{\partial(\rho E)}{\partial t} + \frac{\partial(\rho uEr)}{r\partial r} + \frac{\partial(\rho vE)}{\partial z} = -\frac{\partial(pur)}{r\partial r} - \frac{\partial(pv)}{\partial z} + S_e \quad (4)$$

where ρ is gas density, u and v are the axial and radial velocity, p is pressure, E is the specific total energy, and S_e is the energy source term, respectively.

The energy source term S_e in (4) represents the arc effects on the flow field, which is mainly composed of the joule heating and radiative transfer mechanism [7].

The FVFLIC method is used to solve the conservation equations. It can solve the supersonic flow problem with a moving boundary. The detailed numerical scheme of the FVFLIC method can be found in [3]. The unstructured grid is used and the grid is automatically adjusted according to the moving boundary. The transport and thermodynamic properties of real SF_6 gas are obtained from [8].

To calculate the joule heating, the current density in the arc region should be known. The current density in the conducting arc region is computed using the conservation equation of the electric current and Ohm's law.

$$\nabla \cdot \vec{J} = 0 \quad (5)$$

$$\vec{J} = \sigma \vec{E} \quad (6)$$

where $\vec{J}$ is the electric current density, σ is the electrical conductivity, and $\vec{E}$ is the electric field intensity.

The joule heating and total electric power in the arc region are then calculated as follows:

$$S_{ohm} = \sigma \left|\vec{E}\right|^2 \quad (7)$$

$$W_{arc} = \int S_{ohm}\, dv = \int \sigma \left|\vec{E}\right|^2 dv \quad (8)$$

where $\sigma = \sigma(T, P)$ is function of the local temperature T and pressure P [8].

To emulate the re-absorption of the emitted radiation in the arc edge, the boundary source layer is introduced where the re-absorbed radiation energy is distributed. In the central arc region $0 < r < R_a$ in Fig. 3, most input energy is transferred in the form of the radiation. In the arc boundary region $R_a < r < R_b$, a large amount of the emitted radiation energy is re-absorbed [9].

In this study, a region of concern is not the arc region but the shield and tank region far away from the arc channel. So, the simplified energy source calculation technique is introduced. The energy source term S_e in (4) is calculated considering the joule heating, emission and re-absorption of the radiation energy as follows:

a. Central arc region A ($0 < r < R_a$) :

$$S_e = k_1\, W_{arc} / V_A \quad (9)$$

b. Arc boundary layer B ($R_a < r < R_b$) :

$$S_e = k_2\, (1 - k_1)\, W_{arc} / V_B \quad (10)$$

where $0 < k_1, k_2 < 1$, $k_1 + k_2 < 1$, V_A : volume of region A, V_B : volume of region B.

The constant k_1 is related to the amount of the emitted energy from the central arc region, and k_2 represents the ratio of the re-absorbed energy to the emitted energy. In this study, k_1 is set 0.1, and k_2 0.8, respectively. The proposed empirical arc model can save the computational cost considerably considering the emission and re-absorption of the radiation energy in the arc region.

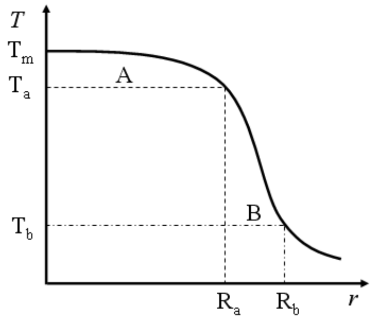

Fig. 3. Definition of central arc region (A) and re-absorption region (boundary source layer, B). T_m : axis temperature, T_a : aT_m , a = 0.83 [9] , T_b : 3,000K.

3. Critical Electric Field Intensity

When an electrical arc is generated between the contacts in the GCB, the hot gas flows through the surrounding structures such as an exhaust tube, a shield or a grounded tank. The dielectric strength of the hot gas is much lower than that of the cold gas. The breakdown voltage of a hot gas can be predicted using the critical electric field intensity (E_{cr}). The E_{cr} is the electric field intensity when the breakdown occurs. Much research has been carried out to calculate the E_{cr}. The E_{cr} is calculated under the local thermal equilibrium condition. Various processes such as elastic collisions, vibration excitations, electronic excitation, dissociation, attachment, and ionization are taken into consideration to evaluate the electron energy distribution function. There are some differences among the published E_{cr} data mainly due to the number of particles considered in the calculation and the interactions between electrons and the different gas dissociation products. We adopted the Yousfi's E_{cr} data [6] because it takes 12 SF_6 dissociated species in the calculations which involve both the electron and ion kinetics, resulting in the most elaborate data available now.

Fig. 4 shows the E_{cr} data used in this study. The values were derived from the E_{cr}/N data calculated by Yousfi [6] as shown in Fig. 5. In [6], not E_{cr} data but E_{cr}/N data were calculated and to know the E_{cr} data, the number density N should be known. The SF_6 properties from [8] are used to obtain the number density N as a function of gas temperature and pressure.

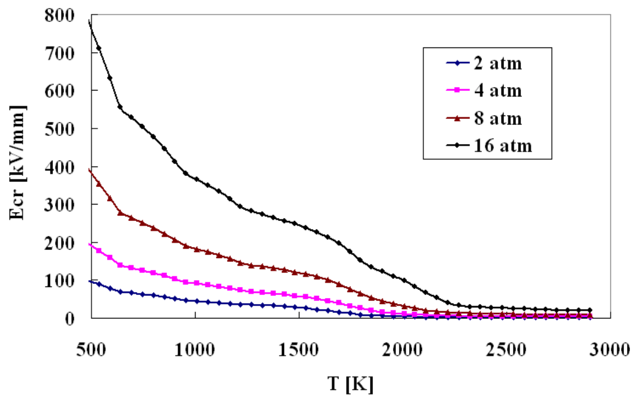

Fig. 4. Critical electric field intensity with respect to temperature and pressure.

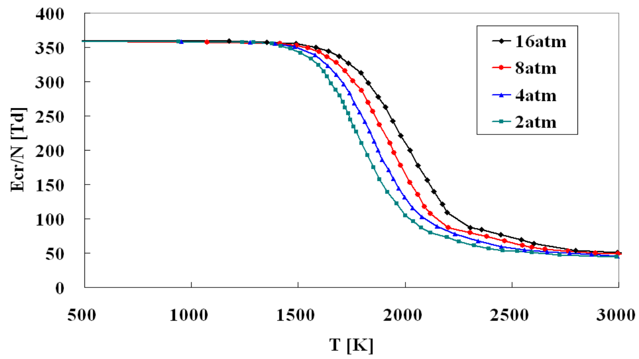

Fig. 5. $(E/N)_c$ data with respect to temperature and pressure.

4. Results and Discussion

From the hot gas flow analysis, the pressure and temperature inside the GCB can be obtained. Then, the E_{cr} can be calculated with Fig. 4 data. The TRV is applied right after the current interruption. With the given TRV, we can calculate the applied electric field intensity $E_{applied}$ everywhere inside the GCB chamber. In this study, $E_{applied}$ is calculated using the finite element method (FEM). If the $E_{applied}$ is greater than the E_{cr}, the probability of breakdown is high. So, we can define the breakdown index as the ratio of $E_{applied}$ to E_{cr}. If this index is greater than 1, the breakdown is predicted.

4.1 Experimental Tests

A dielectric breakdown test was carried out for the 145kV 40kA puffer type GCB. Fig. 6 shows the testing facility in the synthetic test room. The filling SF_6 gas pressure is 6 [bar]. During the test, the interrupting current, the breakdown voltage, and the breakdown instant were recorded. The current wave form is sinusoidal with a frequency of 60Hz. Table 1 shows the testing results with respect to the interrupting current. In the case of $20kA_{rms}$, the arc energy is relatively small and no breakdown was observed. However, in the increased current case of 30 or $35kA_{rms}$, higher arc energy causes a breakdown between a shield and tank. The breakdown voltage for 30 and 35 kA_{rms} is 240kV and 90kV respectively. Fig. 7 shows the scar position formed by the flash-over. It is located near the shield hole.

Fig. 6. Testing facility and 145kV 40kA GCB.

Fig. 7. Position and scar of breakdown.

Table 1. Test results

Current [kA_{rms}]	Arcing time [ms]	TRV peak [kV]	Test result
20	20.0	243	Success
30	20.5	240	Breakdown
35	20.6	99	Breakdown

4.2 Simulation Results

Fig. 8 shows the mesh diagram for the initial and final positions of the moving parts. To consider the moving boundary, the mesh is automatically adapted with respect to geometry changes.

Figs. 9 and 10 show the temperature distribution for the case of $20kA_{rms}$ and $30kA_{rms}$ respectively. The temperature distribution for the $20kA_{rms}$ case shows lower values between a shield and tank compared to the $30kA_{rms}$ case. In the case of $20kA_{rms}$, due to the relatively low arc energy, the temperature after current zero is less than 1,500K between the shield and the tank as shown in Fig. 9 (e). However, in the case of $30kA_{rms}$, the higher temperature (T>1,700K) is shown around the shield region as shown in Fig. 10 (e), which results in the lowered dielectric strength.

The breakdown index which is the ratio of the $E_{applied}$ to the E_{cr} is shown in Fig. 11 for both cases. For a current of $20kA_{rms}$, the index is much lower than one everywhere between a tank and shield. Whereas, in the case of $30kA_{rms}$, the point whose breakdown index is closer to one is shown in Fig. 11 (b). This indicates the higher probability of a breakdown compared to a current of $20kA_{rms}$. During the tests, for a current of $20kA_{rms}$, the GCB interrupted the current successfully, whereas a breakdown occurred for a current of $30kA_{rms}$.

By comparing Fig. 10 (e) and Fig. 11 (b), we can see that the position of the maximum breakdown index is almost the same as that of the highest temperature. The position of the breakdown scar observed in the test is also marked in Fig. 11 (b). It is very difficult to predict the location of the breakdown initiation and the breakdown path. But the simulation result shows that the point of the maximum breakdown index is reasonably located near the observed breakdown scar.

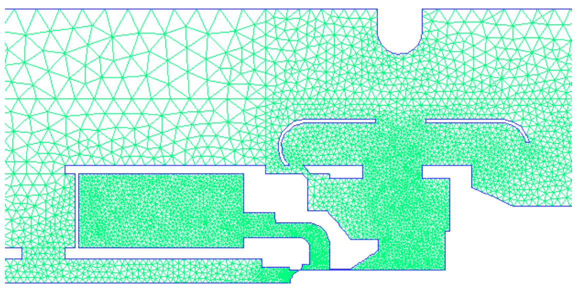

(a) initial position

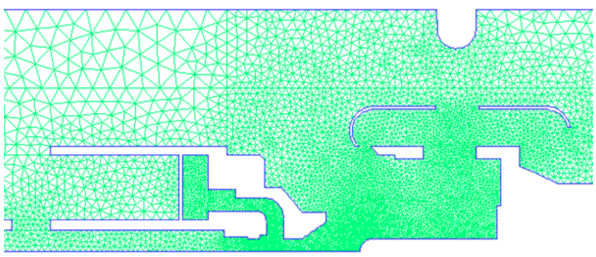

(b) final position

Fig. 8. Mesh diagram used in simulation.

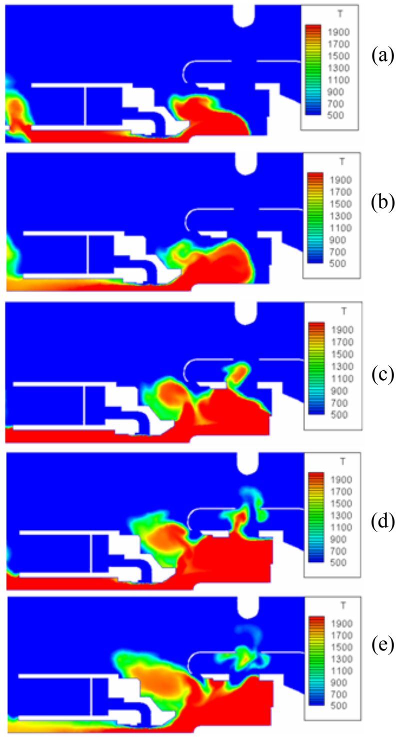

Fig. 9. Temperature distribution in the case of arc current $20kA_{rms}$, arcing time 20.0ms. (a) t = 10ms (b) t = 15ms (c) t = 18ms (d) t = 20ms(current zero) (e) t = 250 μs after current zero.

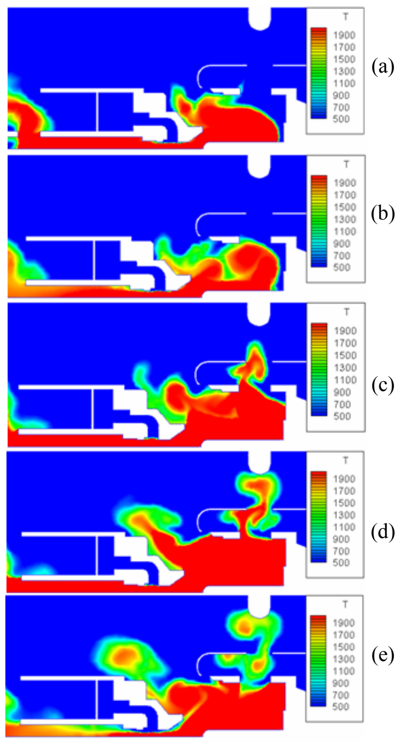

Fig. 10. Temperature distribution in the case of arc current $30kA_{rms}$, arcing time 20.5ms. (a) t = 10ms (b) t = 15ms (c) t = 18ms (d) t = 20.5ms(current zero) (e) t = 250 μs after current zero.

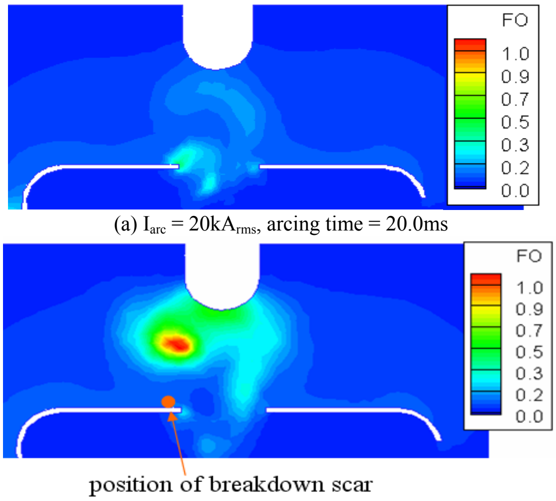

(a) I_{arc} = 20kA_{rms}, arcing time = 20.0ms

(b) I_{arc} = 30kA_{rms}, arcing time = 20.5ms

Fig. 11. Plot of Breakdown index (time = 250 μs after current zero).

5. Conclusion

In this paper, the dielectric characteristics of a hot SF_6 gas in a GCB during a large current interruption have been analyzed. For the computation of hot gas flow, the FVFLIC method is employed considering the real SF_6 gas properties and the moving boundary. The arc region is simulated using the simple energy source term in the energy conservation equation. Such a simple arc representation is adequate to the analysis of hot gas flow around the shield and the tank of a GCB.

Among the several E_{cr} data, Yousfi's data is found to be suitable to the numerical calculation of breakdown criterion. By comparing the $E_{applied}$ and the E_{cr}, the possibility of the breakdown is predicted. The breakdown criterion was applied to the 145kV 40kA GCB and the consistent results between simulation and experiment were confirmed. The amount of hot gas flow between the shield and the tank is crucial to the dielectric characteristics. So, the optimal design of the gas flow passage to reduce the amount of hot gas flow and to cool the hot gas down is necessary for a compact GCB design.

The presented method can indicate the location of a breakdown with considerable accuracy. It can be said that the dielectric breakdown criterion employing the critical electric field is a good means to understand the breakdown of hot SF_6 gas inside a GCB.

References

[1] Y. Hayashi, K. Suzuki, E. Haginomori, H. Toda and H. Ikeda, "On the hot gas exhaustion in the exhaust chamber of a gas circuit breaker after short-circuit current interruption," *J. Phys. D, Appl. Phys.*, Vol. 30, pp. 3123-3130, 1997.

[2] T. Uchii, S. Nishiwaki and S. A. Boggs, "Effects of hot SF_6 on post-arc circuit breaker design," *IEEE Trans. Power Delivery*, Vol. 19, pp. 124-130, Jan. 2004.

[3] Y. Zhao and D. E. Winterbone, "The finite volume FLIC method and its stability analysis," *Int. J. Mesh. Sci.*, Vol. 37, pp. 1147-60, 1995.

[4] G. J. Cliteur, Y. Hayashi, E. Haginomori and K. Suzuki, "Calculation of the uniform breakdown field strength of SF_6 gas," *IEEE Trans. Dielect. Elect. Insulation*, Vol. 5, pp. 843-849, 1998.

[5] M. Yousfi, Ph. Robin-Jouan, Z. Kanzari, "Breakdown Electric Field Calculations of Hot SF_6 for High Voltage Circuit Breaker Applications," *IEEE Trans. on Dielect.Elect. Insulation*, Vol. 12, No. 6, pp. 1192-1200, 2005.

[6] Ph. Robin-Jouan and M. Yousfi, "New Breakdown Electric Field Calculations for SF_6 High Voltage Circuit Breaker Applications," *Proceedings of Gas Discharge and Their Applications* – Xi'an, China, pp. 317-320, 2006.

[7] C. M. Dixon, J. D. Yan and M. T. C. Fang, "A comparison of three radiation models for the calculation of nozzle arcs," *J. Phys. D: Appl. Phys.*, Vol. 37, pp. 3309-3318, 2004.

[8] L. S. Frost and R. W. Liebermann, "Composition and transport properties of SF_6 and their use in a simplified enthalpy flow arc model," *Proc. IEEE*, Vol. 59, pp. 474-485, Apr. 1971.

[9] J. F. Zhang, M. T. C. Fang and D.B. Newland, "Theoretical investigation of a 2kA DC nitrogen arc in a supersonic nozzle," *J. Phys. D: Appl. Phys.*, Vol. 20, pp. 368-379, 1987.

Hong-Kyu Kim was born in Yeongchon, Korea, in 1969. He received his B.Sc. degree in 1995, his M.Sc. degree in 1997 and his Ph.D. degree in 2001 from the School of Electrical Engineering, Seoul National University, Korea. He has been working for the Korea Electrotechnology Research Institute (KERI) since 2001. His research field covers the numerical analysis of electromagnetic fields, and the analysis of cold and hot gas flow in high voltage gas circuit breakers. He is a regular member of CIGRE working group A3.24.

Jin-Kyo Chong was born in Cheorwon, Korea, in 1967. He received his B.S. and M.S. degrees in electrical engineering from Kangwon National University in 1991 and 1994, respectively. Since 1994, he has been with KERI as a research engineer in the power apparatus research center. His research interests are electric and magnetic analysis, high voltage gas circuit breaker design and its breaking capability testing.

Ki-Dong Song was born in ChenAn, Korea, in 1963. He received his B.S. and M.S. degrees in electrical engineering from Inha University in 1988 and 1990, respectively. He received his Ph.D. degree in electrical engineering from Busan National University in 2003. He worked for the Korea Electrotechnology Research Institute (KERI) from 1990 and is now a team leader of the Circuit Breaker Design Team. His research interests focus on analysis and design for circuit breakers and GIS (gas insulated switchgear).